Supplementary

Supplementary Figures

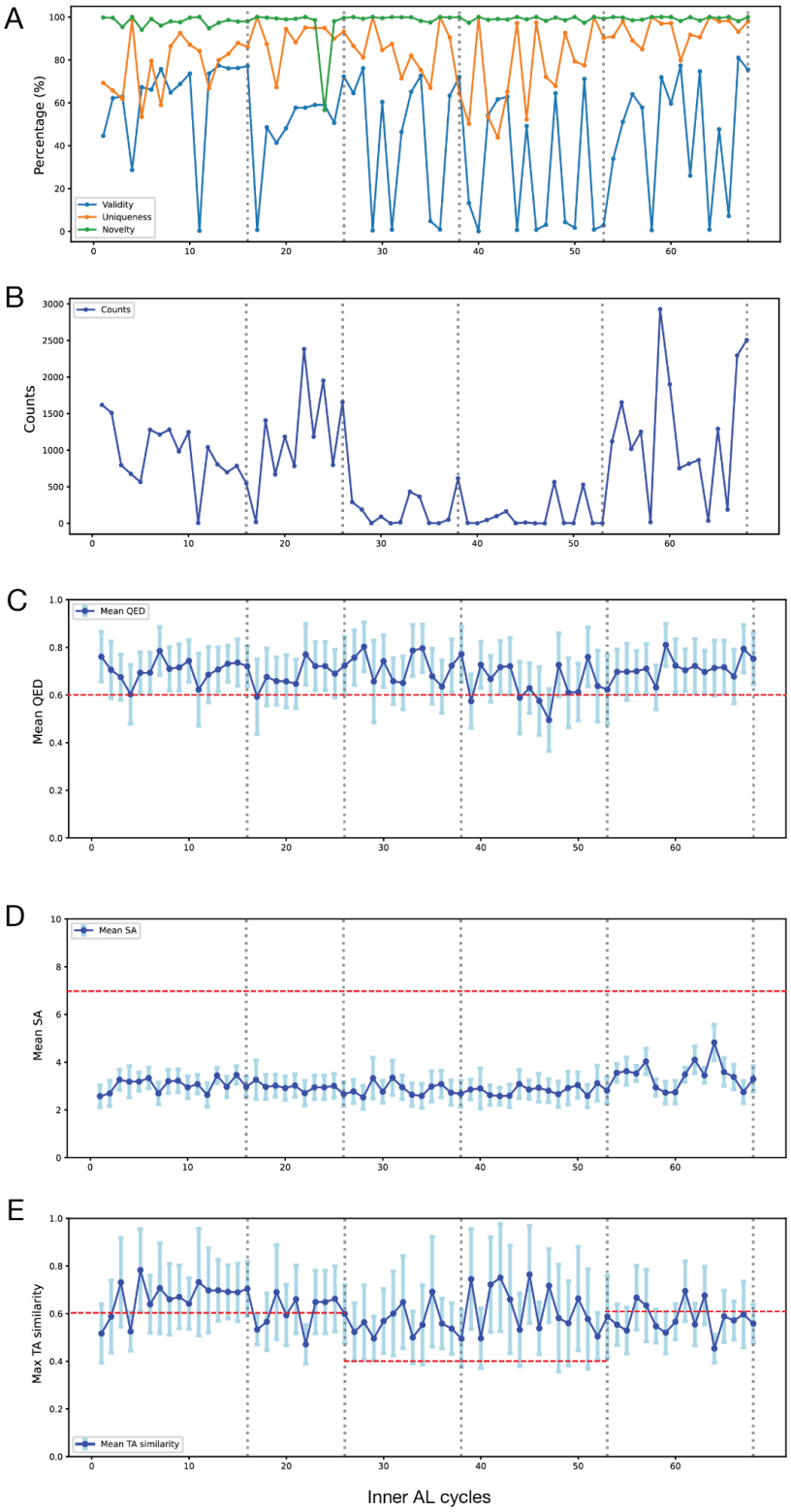

Supplementary Figure 1. Evolution of generation and AL metrics over inner AL cycles for CDK2. A. Validity (percentage of chemically valid molecules among those generated), uniqueness (percentage of non-duplicate valid molecules), and novelty (percentage of unique molecules not found in the temporal-specific set) at each inner AL cycle. **B.** Number of molecules meeting QED, SA, and similarity thresholds at each inner AL cycle. **C–E.** Average QED (C), SA (D), and maximum Tanimoto similarity to molecules in the specific set (E) for valid generated molecules at each inner AL cycle. Standard deviation is shown as vertical light blue lines. Red horizontal dotted lines indicate the property thresholds applied at each outer AL cycle. Vertical dotted lines mark the boundaries between outer AL cycles.

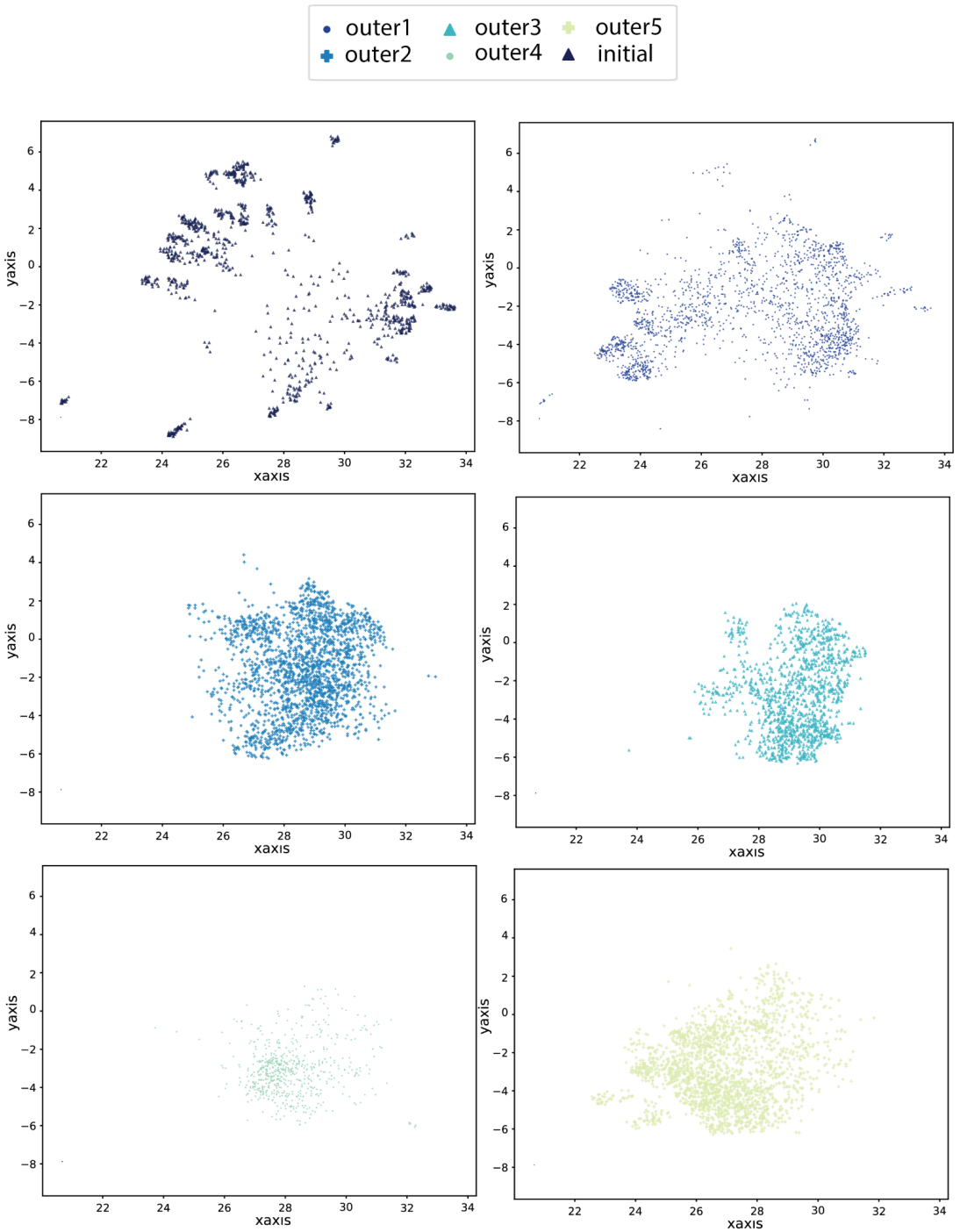

Supplementary Figure 2. UMAP splits by initial-specific set and outer AL cycles CDK2 molecules, with marker styles and colors indicating different cycles as shown in the legend. The initial-specific set is labeled 'initial' and outer AL cycles as 'outerX'.

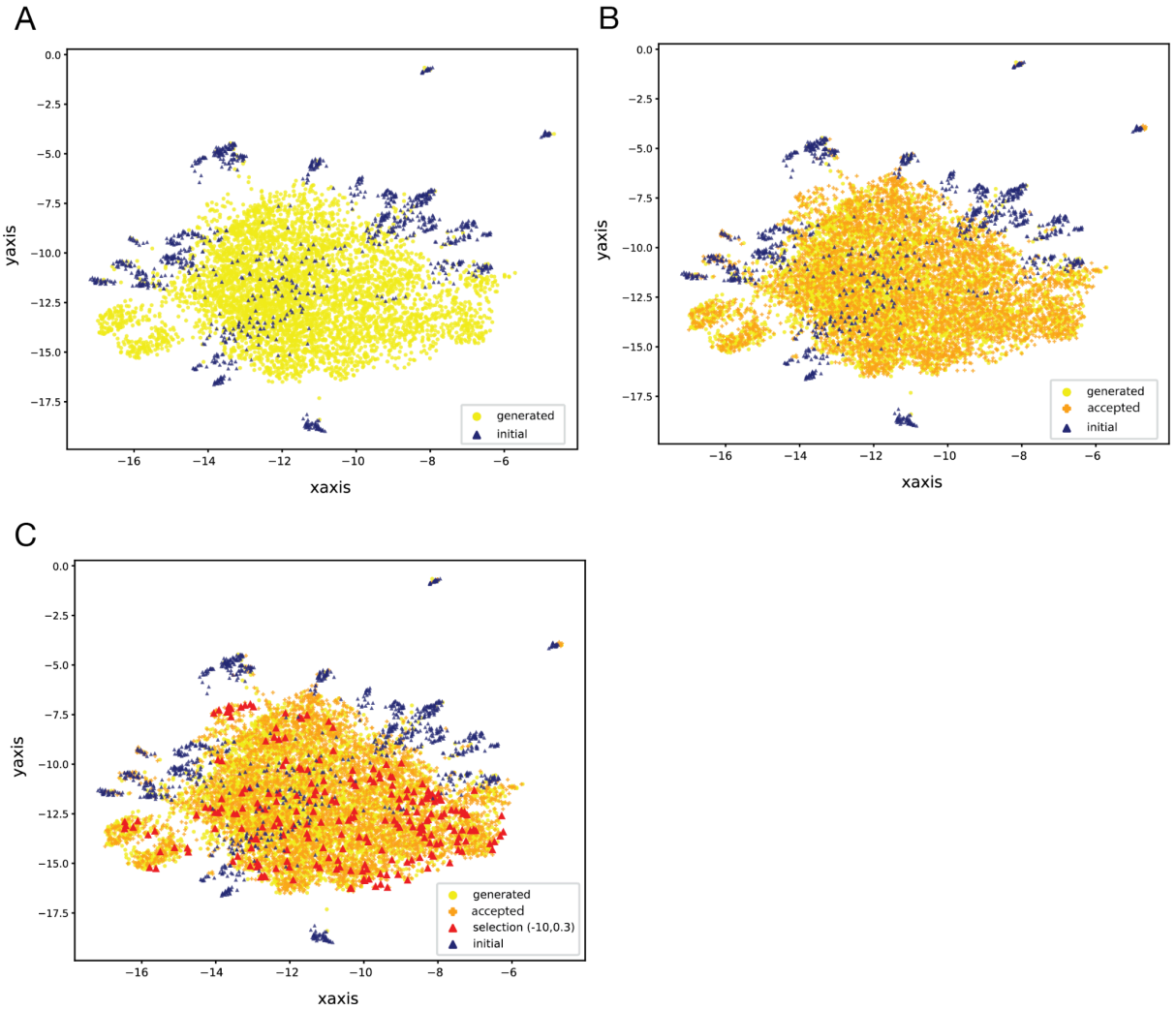

Supplementary Figure 3. UMAP illustrating the GM workflow's chemical space exploration for CDK2. A. UMAP with the generated molecules over the five outer AL cycles (generated) and the molecules of initial-specific set (initial) **B.** UMAP from panel A with outer AL cycle accepted molecules (accepted) highlighted in orange **C.** UMAP from panel B with the position of molecules meeting the candidate selection stringent filters highlighted in red.

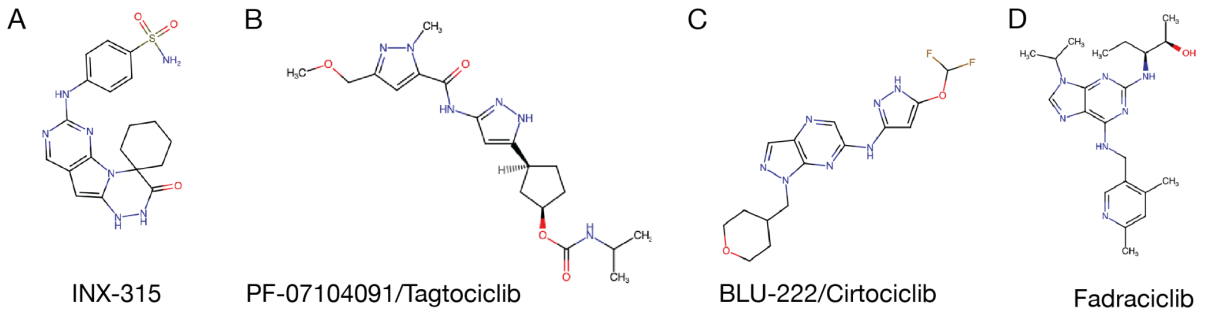

Supplementary Figure 4. A. INX-315, CDK2 inhibitor in Phase 1/2 clinical trials, targeting CCNE1-amplified, platinum-resistant ovarian cancer. **B.** PF-07104091, CDK2 inhibitor in Phase 1/2a clinical trials for patients with advanced or metastatic solid tumors **C.** CDK2 inhibitor in Phase 1 clinical trials as monotherapy for patients with advanced solid tumors, and in combination with ribociclib and fulvestrant for HR+/HER2– breast cancer **D.** Fadraciclib, CDK2/9 inhibitor in Phase 1 clinical trials for patients with advanced solid tumors and lymphoma.

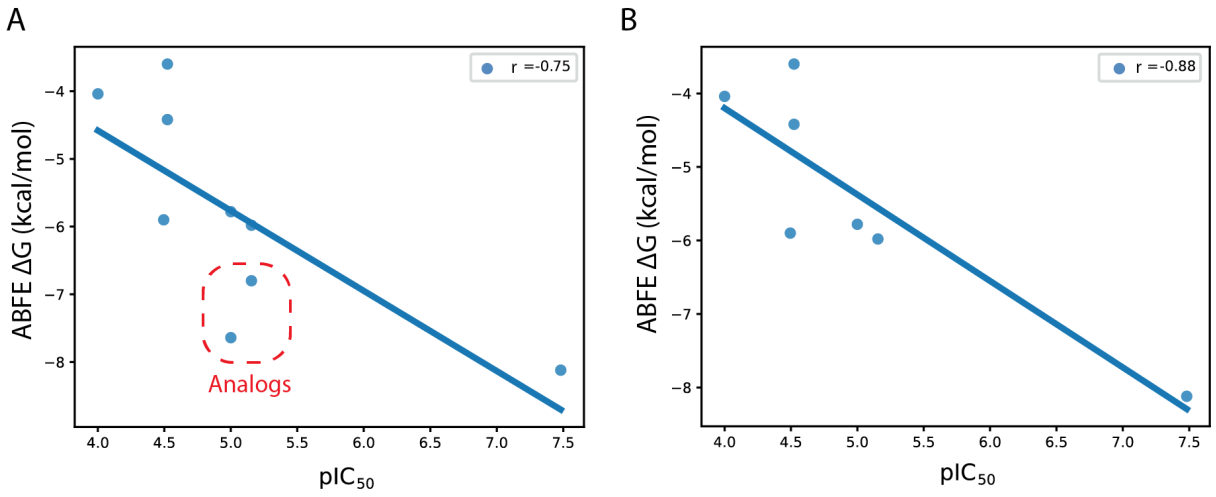

Supplementary Figure 5. Comparison of ABFE ΔG with experimental affinities. A. Linear regression and correlation coefficient between ABFE ΔG and pIC_{50} for the synthetized and experimentally tested new molecules. **B.** Linear regression and correlation coefficient between ABFE ΔG and pIC_{50} for the synthesised and experimentally tested new molecules less the obtained analogs.

Candidate Drugs	Closest Analog	Closest Analog Similarity	Mean Similarity Top10 analogs	#Analogs above 0.5 similarity
outer1_28 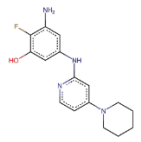	m_270004dcb____14046104____17309876 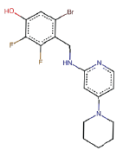	0.544	0.529	23
outer5_137 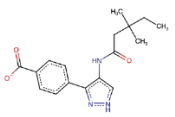	m_11bcb____16803812____6391822 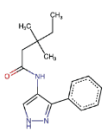	0.750	0.633	107
outer5_105 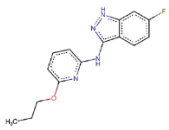	m_270004bcb____12217816____23163454 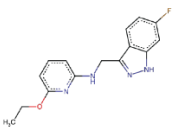	0.596	0.544	31
outer5_28 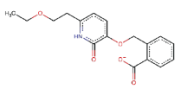	m_279392bbb____26114062____26184930 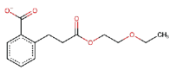	0.481	0.451	0
outer5_193 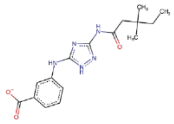	m_188690bbe____7326632____13237134 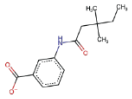	0.654	0.556	15
(R)-outer1_15 / (S)-outer1_15 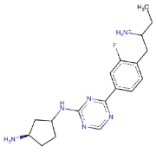	m_276450abb____27870368____14199924____28202694 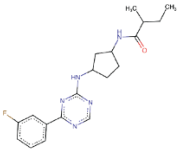	0.473	0.455	0
outer1_5 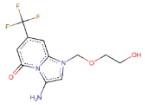	m_34bhb____9817866____11974694 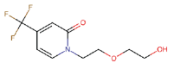	0.451	0.423	0
outer2_74 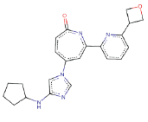	m_282512abb____24322962____24202952 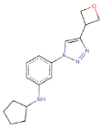	0.365	0.335	0
outer5_41 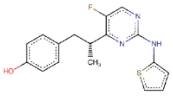	m_27bjd____18058996____18312382 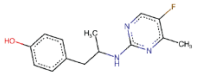	0.466	0.443	0
outer5_125 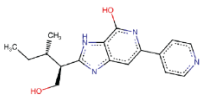	m_22bbo____18901724____25795036 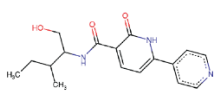	0.460	0.426	0

Supplementary Figure 6. Results of the analog search in Enamine Real Space 76B for CDK2 compounds selected for synthesis.

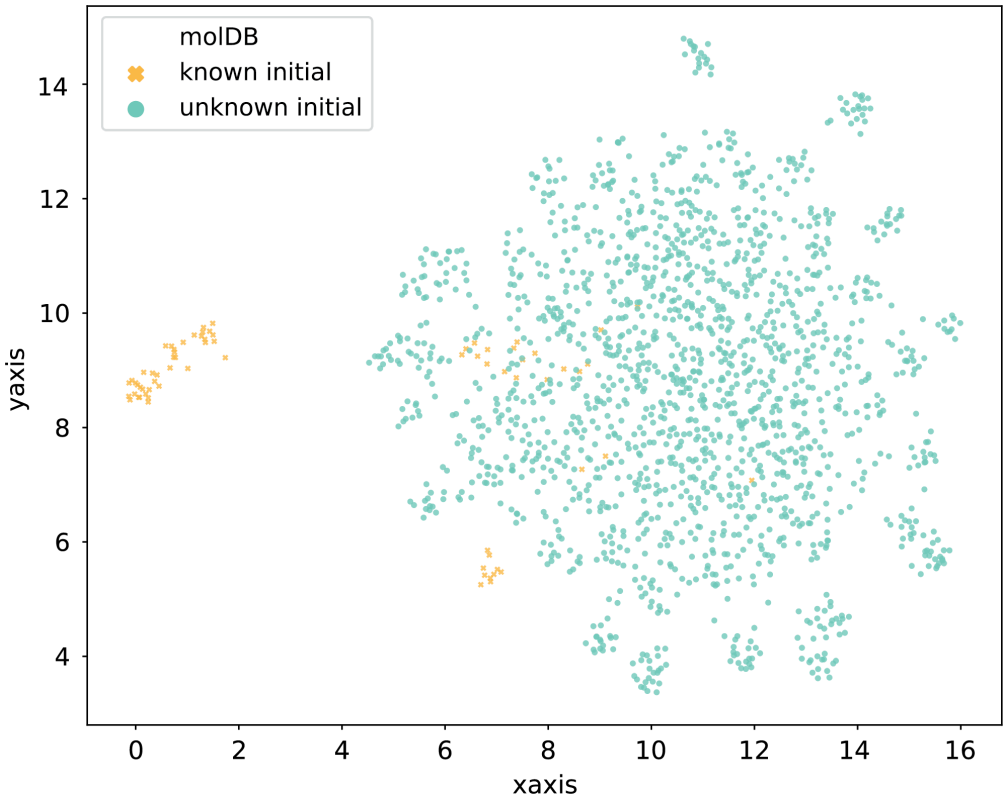

Supplementary Figure 7. UMAP of the molecules from the KRAS known and unknown initial-specific sets.

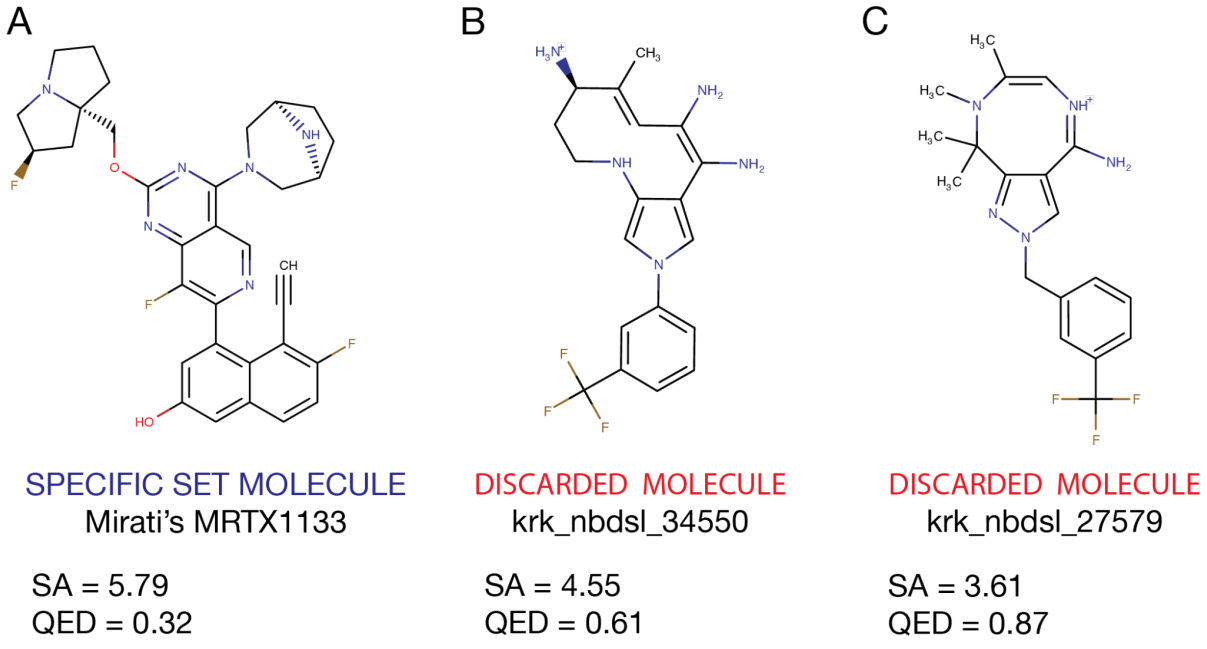

Supplementary Figure 8. MRTX133 Mirati's inhibitor and resulting artifacts from the known generated molecules. A. MRTX1133 $KRAS^{G12D}$ inhibitor. **B.** krk_nbdsl_34550 known generated molecule exemplifying a

discarded molecule due to a broken bicycle **C.** krk_nbdsl_27579 known generated molecule exemplifying a discarded molecule due to a 8-membered ring.

Candidate Drugs	Closest Analog	Closest Analog Similarity	Mean Similarity Top10 analogs	#Analogs above 0.5 similarity
kru_nbdsl_23704 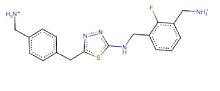	m_270166bbb____17563404____16818318 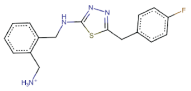	0.717	0.671	1003
kru_nbdsl_15229 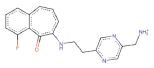	m_27bbh____10891608____12297348 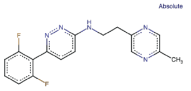	0.391	0.364	0
kru_nbdsl_14271 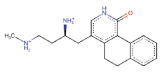	m_272150bbb____9362026____9361304 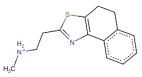	0.313	0.291	0
kru_nbdsl_5803 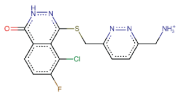	m_207bcb____17627048____23851928 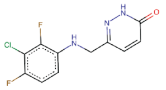	0.333	0.316	0

Supplementary Figure 9. Results of the analog search in Enamine Real Space 76B for KRAS molecules with potential activity against KRAS.

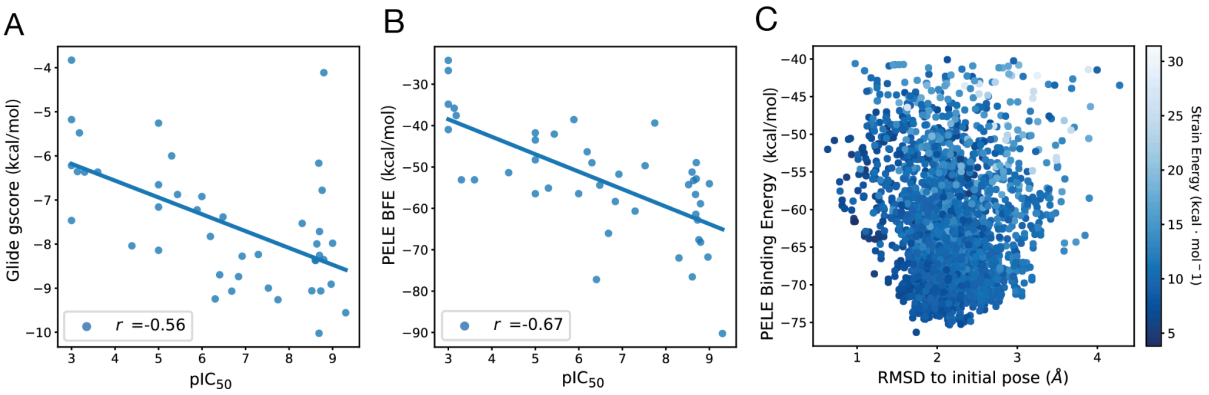

Supplementary Figure 10. Comparison of Glide gscore and PELE BFE with experimental affinities. A. Linear regression and correlation coefficient between Glide gscore and pIC_{50} for a subset of molecules from the initial-specific set of CDK2. **B.** Linear regression and correlation coefficient between PELE's BFE and pIC_{50} for the same subset of molecules from panel A. **C.** Example of a PELE energetic profile used to compute BFE values in panel B.

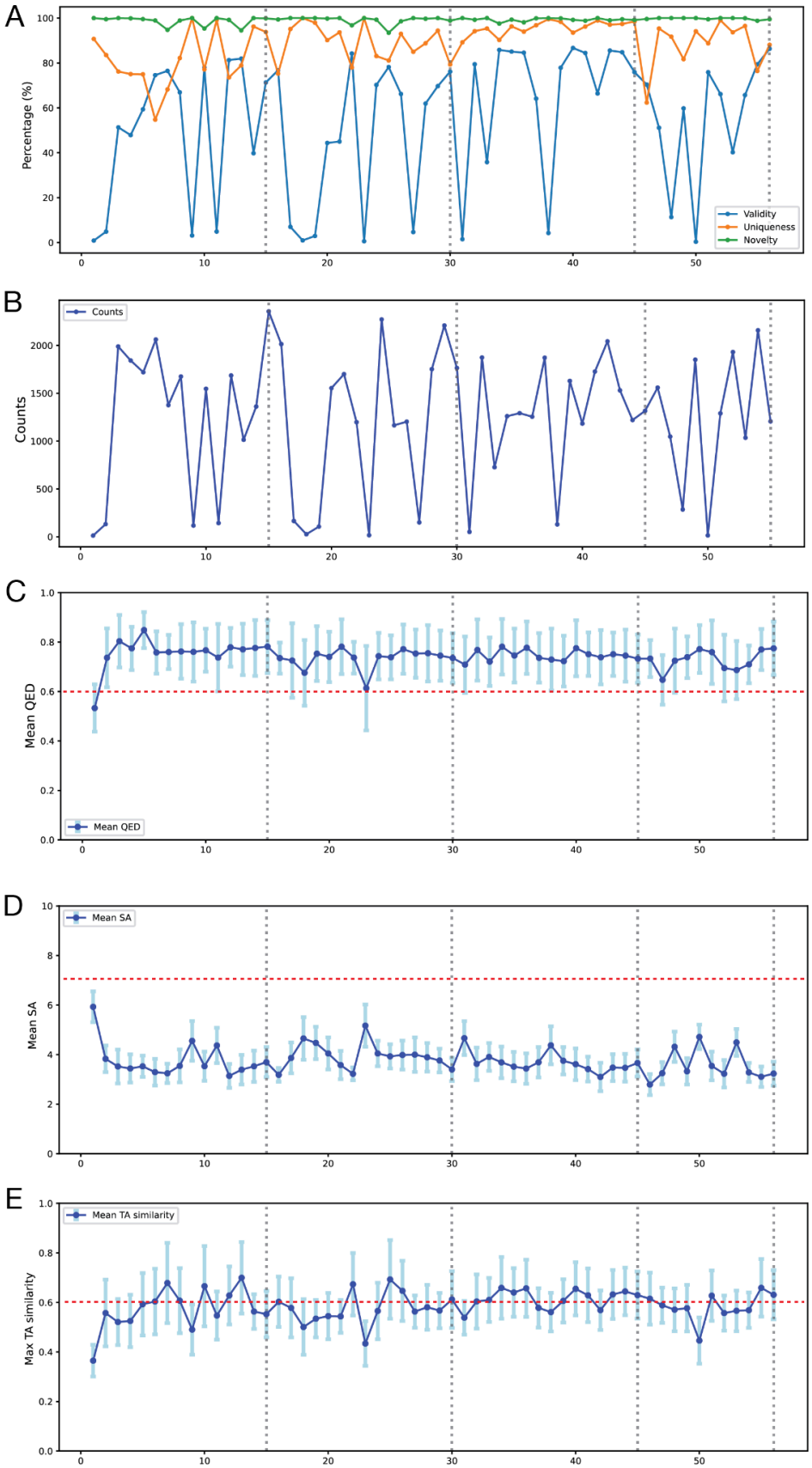

Supplementary Figure 11. Evolution of generation and AL metrics over inner AL cycles for KRAS unknown generation. A. Validity (percentage of chemically valid molecules among those generated), uniqueness (percentage of non-duplicate valid molecules), and novelty (percentage of unique molecules not

found in the temporal-specific set) at each inner AL cycle. **B.** Number of molecules meeting QED, SA, and similarity thresholds at each inner AL cycle. **C–E.** Average QED (C), SA (D), and maximum Tanimoto similarity to molecules in the specific set (E) for valid generated molecules at each inner AL cycle. Standard deviation is shown as vertical light blue lines. Red horizontal dotted lines indicate the property thresholds applied at each outer AL cycle. Vertical dotted lines mark the boundaries between outer AL cycles.

Supplementary Tables

	Outer1	Outer2	Outer3	Outer4	Outer5
Generated	49796	24766	26387	19581	36465
Inner active learning	15068 (30.3%)	12040 (48.6%)	2065 (7.8%)	1446 (7.3%)	18645 (51.1%)
Outer active learning	885 (1.8%)	1192 (4.8%)	167 (0.6%)	88 (0.5%)	2295 (6.3%)

Supplementary Table 1. Total number of CDK2 chemically valid generated molecules accepted by the inner and outer AL cycles.

(Table in the adjacent .xlsx file)

Supplementary Table 2. CDK2 generated molecules meeting the stringent Glide gscore (-10 kcal·mol^{-1}) and maximum similarity to the initial-specific set (0.3) thresholds during the candidate selection phase. The table lists their SMILES, Glide gscore, PELE BFE, maximum similarity (Max. similarity) and their synthesis status as TRUE or FALSE. Successfully synthesized molecules are highlighted in green; unsuccessful ones are highlighted in red.

(Table in the Supplementary Data .xlsx file)

Supplementary Table 3. Affinity values predicted by MM methods (Glide, PELE and ABFE simulations) and affinity values obtained with inhibitory assays for the 10 CDK2 candidate drugs and 3 ABFE CDK2 control molecules (1). The table includes their SMILES, Glide gscore, PELE BFE, maximum similarity to the initial-specific set (Max. similarity), ABFE ΔG, ABFE predicted K_d, experimental IC_{50} (Exp. IC_{50}), experimental ΔG (ΔG=-RTln(Exp. IC_{50})) (Exp. ΔG), and experimental maximum % inhibition from inhibitory assays (Exp. Max. % inhibition). Molecules with a ABFE predicted K_d < 100μ or with an IC_{50} < 50 μM are highlighted in green while the ones above this thresholds are highlighted in red.

(Table in the Supplementary Data .xlsx file)

Supplementary Table 4. Analog search in Enamine Real Space 76B for CDK2 compounds selected for synthesis. The table includes the SMILES and Tanimoto similarity of the 10 closest analogs for each compound, as well as the average Tanimoto similarity across these analogs.

		Outer1	Outer2	Outer3	Outer4
Known	Generated	47875	42039	40303	23248
	Inner active learning	9646 (20.1%)	13370 (31.8%)	14199 (35.2%)	13481 (57.9%)
	Outer active learning	387 (0.8%)	982 (2.3%)	1758 (4.4%)	408 (1.7%)
Unknown	Generated	37143	34452	50127	30343
	Inner active learning	16690 (44.9%)	15543 (45.1%)	17806 (35.6%)	12386 (40.8%)
	Outer active learning	4432 (11.9%)	6175 (17.9%)	7082 (14.1%)	5799 (19.1%)

Supplementary Table 5. Total number of KRAS generated molecules accepted by the inner and outer AL cycles during each generative process (Known and Unknown).

(Table in the Supplementary Data .xlsx file)

Supplementary Table 6. KRAS generated molecules meeting the stringent Glide gscore (-9 kcal·mol^{-1}) and maximum similarity to the unknown specific set (0.25) thresholds during the candidate selection phase. The table lists their SMILES, Glide gscore, PELE BFE, maximum similarity (Max. similarity), net charge and their ABFE status as TRUE or FALSE. Molecules wich went through an ABFE simulation are highlighted in green.

(Table in the Supplementary Data .xlsx file)

Supplementary Table 7. Affinity values predicted by MM methods (Glide, PELE and ABFE simulations) for the 19 KRAS candidate drugs and 4 ABFE KRAS control molecules (2). The table includes their SMILES, Glide gscore, PELE BFE, maximum similarity to the unknown specific set (Max. similarity), ABFE ΔG, ABFE predicted K_d, experimental IC_{50} (Exp. IC_{50}), experimental K_d (Exp. K_d), and experimental ΔG (ΔG=-RTln(exp. K_d)) (Exp. ΔG). Molecules with a ABFE predicted K_d < 100μ or with an IC_{50} < 50 μM are highlighted in green while the ones above this thresholds are highlighted in red.

(Table in the Supplementary Data .xlsx file)

Supplementary Table 8. Analog search in Enamine Real Space 76B for molecules with potential activity against KRAS. The table includes the SMILES and Tanimoto similarity of the 10 closest analogs for each compound, as well as the average Tanimoto similarity across these analogs.

Supplementary Methods

Compound Synthesis

The synthesis of the CDK2 generated molecules was performed by Enamine LTD.

General Experimental Procedures

Solvent Purification: Solvents were purified following standard procedures as described by Armarego, W. L. F.; Chai, C. Purification of Laboratory Chemicals, 5th ed.; Elsevier: Oxford, U.K., 2003

Melting Points: Melting points were determined using an automated melting point system.

Thin-Layer Chromatography (TLC): Analytical TLC was conducted on silica gel plates. Column chromatography was performed using silica gel (230–400 mesh) as the stationary phase.

Nuclear Magnetic Resonance (NMR) Spectroscopy: ^{1}H, ^{13}C, and ^{19}F NMR spectra were recorded on Varian Unity Plus 400 MHz, Bruker AVANCE DRX 500 MHz, Bruker AVANCE III 400 MHz, or Varian VNMRS 500 MHz spectrometers. Operating frequencies were 500 MHz for ^{1}H, 126 MHz for ^{13}C, and 470 MHz or ^{19}F, or 400 MHz for ^{1}H, 101 MHz for ^{13}C, and 376 MHz for ^{19}F. Chemical shifts are reported in parts per million (ppm) relative to TMS as the internal standard.

Mass Spectrometry (MS): Mass spectra were acquired using various Agilent LC/MSD systems, including:

- Agilent 1100 Series LC/MSD system with DAD/ELSD Alltech 2000ES and Agilent LC/MSD VL G1956B, SL G1956B.
- Agilent 1200 Series LC/MSD system with DAD/ELSD Alltech 3300 and Agilent LC/MSD G6130A, G6120B.
- Agilent 1260 Infinity LC/MSD system with DAD/ELSD Alltech 3300 and Agilent LC/MSD G6120B.
- Agilent 1260 Infinity II LC/MSD system with DAD/ELSD G7102A 1290 Infinity II and Agilent LC/MSD G6120B.

Preparative Chromatography: Preparative flash chromatography was performed using 40 g columns on an Agilent 1260 Infinity system equipped with DAD at 200 nm (DAD1A) and 215 nm (DAD1B), and single quadrupole AP-ESI mass spectrometry detection.

Synthetic scheme and characterization of A-outer5_137

Synthesis of 4-[4-(3,3-dimethylpentanamido)-1-(oxan-2-yl)-1H-pyrazol-3-yl]benzoic acid (A-outer5_137): N-[3-Bromo-1-(oxan-2-yl)-1H-pyrazol-4-yl]-3,3-dimethylpentanamide (170 mg, 474 µmol) was reacted with [4-(methoxycarbonyl)phenyl]boronic acid (171 mg, 95 µmol) in dioxane (1 mL) and water (0.5 mL), using tri-potassium phosphate (403 mg, 1.9 mmol) as a base and

(1,1'-bis(diphenyl-phosphino)ferrocene)dichloropalladium-dichloromethane (65 mg, 95 µmol) as the catalyst. The reaction mixture was purged with argon for 3 minutes and stirred at 80 °C for 48 hours. Upon completion, the mixture was poured into water, acidified to pH=1, and extracted with CH_2Cl_2 (3x). The combined organic extracts were dried over sodium sulfate and concentrated in vacuo. The crude product was purified by HPLC using a water/acetonitrile/0.1% formic acid gradient (0-2-8 min: 23-30-45%) at 30 mL·min^{-1} (loading pump 4 mL water), targeting a product with mass 399. This process yielded 5 mg at 3% of A-outer5_137.

Characterization included ^{1}H NMR (500 MHz, Acetonitrile-d_3), which showed peaks consistent with the compound's structure: δ 8.06 (d, *J*=7.6 Hz, 3H), 7.84 - 7.75 (m, 3H), 5.39 (dd, *J*=10.0, 2.2 Hz, 1H), 4.03 (d, *J*=11.8 Hz, 1H), 3.71 (td, *J*=11.1, 3.2 Hz, 1H), 1.85 (d, *J*=3.4 Hz, 2H), 1.80 - 1.55 (m, 4H), 1.41 (q, *J*=7.4 Hz, 2H), 1.02 (s, 6H), 0.90 (t, *J*=7.5 Hz, 3H). Mass spectrometry confirmed m/z=400.2 [M+H]+.

Synthetic scheme and characterization of outer5_105

Synthesis of 6-fluoro-N-(6-propoxypyridin-2-yl)-1H-indazol-3-amine (outer5_105) through multiple steps: **(1)** To a solution of propan-1-ol (3.22 g, 53 mmol) in THF (40 mL), sodium hydride (1.18 g, 49 mmol) was added in portions and the mixture was stirred at room temperature for 1 h, and 6-fluoropyridin-2-amine (5.0 g, 44 mmol) was added. The resulting mixture was stirred at 70 °C for 16 h. The reaction mixture was cooled and concentrated in *vacuo*. The residue was diluted with water (20 mL) and extracted with EtOAc (2 × 30 mL). The combined organic extracts were washed with water (20 mL), dried over Na_2SO_4, filtered, and evaporated under reduced pressure. The residue was purified by flash column chromatography (gradient MTBE in hexane from 0 to 100%) to give 6-propoxypyridin-2-amine (**cpd1**) (2.9 g, 43%). **(2)** 6-fluoro-3-iodo-1H-indazole (1.05 g, 4.0 mmol) was reacted with 3,4-dihydro-2H-pyran (371 mg, 4.41 mmol) in acetonitrile with catalytic p-TSA (76 mg, 401 µmol) at room temperature for 16h. The resulting mixture was concentrated in *vacuo.* A 5% solution of $NaHCO_3$ in water (20 mL) was added to the residue and the mixture was extracted with DCM (2 × 40 mL). The combined organic extracts were dried over Na_2SO_4, filtered, and concentrated in *vacuo*. The residue was purified by flash column chromatography (gradient MTBE in Hexane from 0 to 100%) to give 6-fluoro-3-iodo-1-(oxan-2-yl)-1*H*-indazole (**cpd2**) (844 mg, 61%). **(3)** Subsequently, a palladium-catalyzed cross-coupling reaction was conducted between **cpd2** (844 mg, 2.44 mmol) and **cpd1** (408 mg, 2.68 mmol) in dioxane (12.5mL) with cesium carbonate (1.59 g, 4.88 mmol), [5-(diphenylphosphanyl)-9,9-dimethyl-9H-xanthen-4-yl]diphenylphosphane (282 mg, 488 µmol), and tris(1,5-diphenylpenta-1,4-dien-3-one)dipalladium (223 mg, 244 µmol). The mixture was evacuated and flushed with argon (3x) and the reaction mixture was heated at 100 °C overnight. The resulting mixture was cooled, diluted with water (50 mL), and extracted with EtOAc (2 × 50 mL). The combined organic extracts were washed with brine (50 mL), dried over Na_2SO_4, filtered, and

evaporated under reduced pressure. The residue was purified by flash column chromatography (gradient MTBE in Hexane from 0% to 100%) to give 6-fluoro-1-(oxan-2-yl)-*N*-(6-propoxypyridin-2-yl)-1*H*-indazol-3-amine (**cpd3**) (580 mg, 64%). **(4)** Finally, to a solution of **cpd3** (300 mg, 810 µmol) in MeOH (1.2 mL), a solution of dioxane/HCl (1.2 mL) was added. The reaction mixture was stirred at RT for 16 h. The resulting mixture was concentrated under reduced pressure, and the residue was purified by HPLC using a water/acetonitrile/0.1% formic acid gradient (0-2-8 min: 43-50-70%) at 30 mL·min^{-1} (loading pump 4 mL CH_3CN). This process yielded 64 mg at 38% of outer5_105.

Characterization included ^{1}H NMR (500 MHz, DMSO-*d*6), which showed peaks consistent with the compound's structure: δ 12.26 (s, 1H), 9.38 (s, 1H), 8.06 (dd, *J*=8.9, 5.3 Hz, 1H), 7.54 (t, *J*=7.9 Hz, 1H), 7.38 (d, *J*=7.9 Hz, 1H), 7.13 (dd, *J*=9.8, 2.3 Hz, 1H), 6.87 (td, *J*=9.2, 2.3 Hz, 1H), 6.19 (d, *J*=7.9 Hz, 1H), 4.13 (t, *J*=6.7 Hz, 2H), 1.68 (h, *J*=7.1 Hz, 2H), 0.92 (t, *J*=7.4 Hz, 3H). Mass spectrometry confirmed m/z=287.2 [M+H]+.

Synthetic scheme and characterization of outer5_28

Synthesis of 2-([6-(2-ethoxyethyl)-2-oxo-1,2-dihydropyridin-3-yl]oxymethyl)benzoic acid (outer5_28) through multiple steps: **(1)** Initially, 2-chloro-6-iodopyridin-3-ol (2.45 g, 9.61 mmol) was reacted with dipotassium carbonate (1.99 g, 14.4 mmol) and methyl 2-(bromomethyl)benzoate (2.41 g, 10.57 mmol) in DMF (30 mL) at 60 °C for 16h. The resulting mixture was poured in water (50 mL) and extracted with EtOAc (3 × 45 mL). The combined organic extracts were washed with a saturated sodium chloride solution (3x), dried over sodium sulfate, and concentrated in vacuum to give methyl 2-[(2-chloro-6-iodopyridin-3-yl)oxy]methylbenzoate (**cpd4**) (3.6 g, 88%). **(2)** In the subsequent step, sodium hydrogen carbonate (1.52 g, 18.1 mmol) was dissolved in a mixture of water (12 mL) and dioxane (30 mL). **Cpd4** (3.65 g, 9.0 mmol), 2-[(E)-2-ethoxy-ethenyl]-4,4,5,5-tetramethyl-1,3,2-dioxaborolane (1.97 g, 9.95 mmol, 1.1 equiv.), and (1,1'-bis(diphenylphosphino)ferrocene)dichloropalladium-dichloromethane (617 mg, 904 µmol) were then added sequentially to the solution. The reaction vessel was evacuated and backfilled with argon (3x) and stirred for 18h at 90 °C. The resulting mixture was poured into water (20 mL) and extracted with EtOAc (3x), the combined organic extracts were dried over sodium sulfate and concentrated in vacuum. The crude product was purified by flash chromatography (MTBE: Hexane gradient from 0 to 100) to obtain methyl 2-[(2-chloro-6-[(1*E*)-2-ethoxyethenyl]pyridin-3-yloxy)methyl]benzoate (**cpd5**) (1.5 g, 48%). **(3)** Subsequently, **cpd5** (500 mg, 1.44 mmol) was dissolved in EtOAc (40 mL) and platinum (2.8 mg, 14 µmol, 0.01 equiv.) was added in portions. The reaction mixture was degassed and stirred for 80h under a hydrogen atmosphere. The resulting mixture was filtered and washed three times with EtOAc and concentrated in vacuum to give methyl 2-([2-chloro-6-(2-ethoxyethyl)pyridin-3-yl]oxymethyl)benzoate (450 mg, 76%) (**cpd6**). **(4)**

In the final step, **cpd6** (450 mg, 1.29 mmol) was dissolved in a mixture of dioxane (6 mL) and water (6 mL). Potassium hydroxide (216 mg, 3.86 mmol), (1E,4E)-1,5-diphenylpenta-1,4-dien-3-one (30 mg, 128 µmol), and di-tert-butyl-[2',4',6'-tris(propan-2-yl)-[1,1'-biphenyl]-2-yl]phosphane (109 mg, 257 µmol) were then added gradually. The reaction mixture was purged with argon and stirred for 16h at 90°C. Afterward, the mixture was cooled, poured into water (20 mL), and washed with EtOAc (3×). The aqueous layer was then acidified to pH=1 and extracted with DCM (3×). The combined organic extracts were dried over sodium sulfate and concentrated in vacuo. The crude product was purified by HPLC using a water/acetonitrile/0.1% formic acid gradient (0-2-8 min: 0-50%) at 30 mL·min^{-1} (loading pump 4 mL ACN), targeting a product with mass 318. This process yielded 16 mg at 4% of outer5_28.

The compound was characterized by ^{1}H NMR (500 MHz, DMSO-d6), which showed peaks consistent with the compound's structure: δ 13.02 (s, 1H), 11.54 (s, 1H), 7.91 (dd, J=7.8, 1.4 Hz, 1H), 7.65 (d, J=7.8 Hz, 1H), 7.59 (td, J=7.5, 1.5 Hz, 1H), 7.46 - 7.39 (m, 1H), 6.75 (d, J=7.4 Hz, 1H), 5.90 (d, J=7.4 Hz, 1H), 5.31 (s, 2H), 3.53 (t, J=6.7 Hz, 2H), 3.39 (q, J=7.0 Hz, 2H), 2.59 (t, J=6.7 Hz, 2H), 1.06 (t, J=7.0 Hz, 3H). Mass spectrometry confirmed m/z=318.2 [M+H]+.

Synthetic scheme and characterization of A-outer5_28

Synthesis of 2-([2-chloro-6-(2-ethoxyethyl)pyridin-3-yl]oxymethyl)benzoic acid (A-outer5_28): **Cpd6** (52 mg, 149 µmol), obtained from the synthetic scheme of outer5-28, was dissolved in a mixture of dioxane (2 mL) and water (2 mL), followed by the addition of potassium hydroxide (25 mg, 447 µmol) in portions. The reaction mixture was purged with argon and stirred for 16h at 90°C. The resulting mixture was cooled, poured into water (20 mL), and washed with EtOAc (3x). The aqueous layer was acidified to pH=1, extracted with DCM (3x), and the combined organic extracts were dried over sodium sulfate and concentrated in vacuo. The crude product was purified by HPLC using a water/acetonitrile/0.1% formic acid gradient (0-1.3-7.3 min: 27-35-45%) at 30 mL·min^{-1} (loading pump 4 mL ACN), targeting a product with mass 335. This process yielded 4 mg at 7% of A-outer5_28.

The compound was characterized by ^{1}H NMR (600 MHz, DMSO-d6) which showed peaks consistent with the compound's structure: δ 13.10 (bs, 1H), 7.94 (d, *J*=7.6 Hz, 1H), 7.66 (d, *J*=7.7 Hz, 1H), 7.62 (t, *J*=7.4 Hz, 1H), 7.50 – 7.43 (m, 2H), 7.25 (d, *J*=8.2 Hz, 1H), 5.53 (s, 2H), 3.63 (t, *J*=6.7 Hz, 2H), 3.40 (q, *J*=7.0 Hz, 2H), 2.85 (t, *J*=6.7 Hz, 2H), 1.05 (t, *J*=7.0 Hz, 3H). Mass spectrometry confirmed m/z=336.0 [M+H]+.

Synthetic scheme and characterization of (R)-outer1_15 and (S)-outer1_15

Synthesis of rac-(1R,3S)-N1-4-[4-(2-aminobutyl)-3-fluorophenyl]-1,3,5-triazin-2-ylcyclopentane-1,3-diamine ((R)-outer1_15) and rac-(1R,3R)-N1-4-[4-(2-aminobutyl)-3-fluorophenyl]-1,3,5-triazin-2-ylcyclopentane-1,3-diamine ((S)-outer1_15): **(1)** Morpholine (12.93 g, 148 mmol) and acetic acid (8.92 g, 148 mmol) were dissolved in toluene (300 mL), followed by the dropwise addition of 1-nitropropane (19.84 g, 222.83 mmol, 1.5 equiv.) and 4-bromo-2-fluorobenzaldehyde (30.0 g, 148 mmol). The mixture was refluxed with a Dean-Stark apparatus for 16h. After cooling, it was poured into water, extracted with EtOAc (3×), washed with saturated sodium chloride solution, dried over sodium sulfate, and concentrated in vacuo. Flash chromatography (methyl tert-butyl ether:hexane, 0-100% gradient) purified the crude material, yielding 4-bromo-2-fluoro-1-[(1Z)-2-nitrobut-1-en-1-yl]benzene (**cpd7**) (6.0 g, 15%) **(2) cpd7** (6.0 g, 22 mmol) was dissolved in dioxane (60 mL) and EtOH (30 mL), cooled to 0 °C, and treated with sodium borohydride (1.87 g, 49.2 mmol) added portionwise. After stirring at room temperature for 2 h, the reaction mixture was diluted with water, extracted with DCM (3×), dried over sodium sulfate, and concentrated in vacuo to yield 4-bromo-2-fluoro-1-(2-nitrobutyl)benzene (**cpd8**) (4.5 g, 67%). **(3) cpd8** (4.5 g, 16 mmol) was dissolved in glacial acetic acid (40 mL), then iron (9.12 g, 163 mmol) was added portion wise. The reaction mixture was refluxed for 3 h, filtered through thin layer of celite, washed with acetic acid (3x), and concentrated in vacuo. TThe residue was dissolved in water, adjusted to pH 14 with sodium carbonate, and extracted with EtOAc (3×). The combined organic layers were dried over sodium sulfate and concentrated in vacuo to yield 1-(4-bromo-2-fluorophenyl)butan-2-amine (**cpd9**) (2.1 g, 50%). **(4) cpd9** (1.69 g, 7.75 mmol) and triethylamine (1.57 g, 15.5 mmol) were dissolved in DCM (30 mL), followed by the portionwise addition of di-tert-butyl dicarbonate (1.69 g, 7.75 mmol). The mixture was stirred at room temperature for 16 h, diluted with saturated sodium hydrosulfate solution, and extracted with DCM. The organic layer was dried over sodium sulfate and concentrated in vacuo to yield tert-butyl N-[1-(4-bromo-2-fluorophenyl)butan-2-yl]carbamate (**cpd10**) (2.5 g, 88%). **(5) cpd10** (2.5 g, 7.22 mmol), 4,4,5,5-tetramethyl-2-(4,4,5,5-tetramethyl-1,3,2-dioxaborolan-2-yl)-1,3,2-dioxaborolane (2.2 g, 8.67 mmol) (1,1'-bis(diphenylphosphino)ferrocene)dichloropalladium-dichloromethane (1:1) (492 mg, 722 µmol) and acetic acid (1.99 g, 21.7 mmol) were dissolved in dioxane (50 mL). The mixture was purged with argon and refluxed for 16 h, then poured into water and extracted with EtOAc (3×). The combined organic extracts were washed with saturated chloride solution, dried over sodium sulfate, and concentrated in vacuo. The crude product was purified by flash chromatography (methyl tert-butyl ether:hexane gradient 0-100%) to yield tert-butyl N-1-[2-fluoro-4-(4,4,5,5-tetramethyl-1,3,2-dioxaborolan-2-yl)phenyl]-butan-2-yl-carbamate (**cpd11**) (2.2 g, 70%). **(6)**

2,4-Dichloro-1,3,5-triazine (206 mg, 1.38 mmol) was dissolved in DCM (30 mL) and cooled to -10 °C. A solution of tert-butyl N-(3-aminocyclopentyl)carbamate (252 mg, 1.26 mmol) and

diisopropylethylamine (195 mg, 1.51 mmol) in DCM (30 mL) was added dropwise over 1h. The mixture was stirred at -10 °C for 1 h, then warmed to room temperature and stirred for another hour. The reaction mixture was washed with water, dried over sodium sulfate, and concentrated in vacuo. The crude product was washed with MTBE, and the filtrate was concentrated in vacuo to yield tert-butyl N-3-[(4-chloro-1,3,5-triazin-2-yl)amino]cyclopentylcarbamate (**cpd12**) (319 mg, 56%). **(7)** Sodium hydrogen carbonate (171 mg, 2.04 mmol) was dissolved in a water (1.5 mL) and dioxane (4 mL) mixture. **cpd11** (400 mg, 1.02 mmol) was added dropwise, followed by **cpd12** (319 mg, 1.02 mmol) in dioxane (3 mL) and 1,1′-bis(diphenylphosphino)ferrocene]-dichloropalladium(II) complex (69 mg, 102 µmol). The mixture was purged with argon for 3 minutes and stirred at 90 °C for 16h. After cooling, the mixture was poured into water, extracted with EtOAc (2X), and the organic layers were washed with water, dried over sodium sulfate, and concentrated in vacuo. Purification by HPLC using a ACN/H_2O gradient (0-1.3-7.3 min: 43-50-65%) at 30 mL·min^{-1} (loading pump 4 mL ACN), targeting a product with mass 545 yielded two isomers: rac-tert-butyl N-[(1R,3S)-3-(4-[4-(2-[(tert-butoxy)carbonyl]aminobutyl)-3-fluorophenyl]-1,3,5-triazin-2-ylamino)cyclopentyl]carbamate (**cpd13**) (48 mg, 9%) and rac-tert-butyl N-[(1R,3R)-3-(4-[4-(2-[(tert-butoxy)carbonyl]aminobutyl)-3-fluorophenyl]-1,3,5-triazin-2-ylamino)cyclopentyl]carbamate (**cpd14**) (32 mg, 6%). **(8) cpd13** (48 mg, 88 µmol) was dissolved in MeOH (5 mL), and dioxane/HCl (1 mL) was added dropwise. The mixture was stirred at room temperature for 16h. After the reaction, the crude product was purified by HPLC using a water/acetonitrile gradient (0-1.3-7.3 min: 0-0-25%) at 30 mL/min (loading pump 4 mL H_2O), targeting a product with mass 344. This process yielded rac-(1R,3S)-N1-4-[4-(2-aminobutyl)-3-fluorophenyl]-1,3,5-triazin-2-ylcyclopentane-1,3-diamine ((R)-outer1_15) as the bis-HCl salt (20 mg, 65%). **(9) cpd14** (32 mg, 58 µmol) was dissolved in MeOH (5 mL), and dioxane/HCl (1 mL) was added dropwise. The mixture was stirred at room temperature for 16h. The crude product was purified by HPLC using a water/acetonitrile gradient (0-1.3-7.3 min: 0-0-25%) at 30 mL·min^{-1} (loading pump 4 mL H_2O), targeting a product with mass 344. This process yielded **ac-(1R,3R)-N1-4-[4-(2-aminobutyl)-3-fluorophenyl]-1,3,5-triazin-2-ylcyclopentane-1,3-diamine** ((S)-outer1_15) as the bis-HCl salt (11 mg, 22%).

Characterization of (R)-outer1_15 included ^{1}H NMR (500 MHz, DMSO-*d*6), which showed peaks consistent with the compound's structure: δ 8.63 (d, *J*=40.4 Hz, 1H), 8.44 (d, *J*=7.1 Hz, 1H), 8.29 - 7.93 (m, 7H), 7.54 (t, *J*=7.8 Hz, 1H), 4.34 (dq, *J*=52.9, 7.2 Hz, 2H), 3.62 - 3.45 (m, 1H), 3.10 - 2.89 (m, 2H), 2.43-2.37 (m, 1H), 2.07 - 1.89 (m, 2H), 1.75 (tt, *J*=10.1, 5.4 Hz, 2H), 1.67 - 1.45 (m, 3H), 0.91 (t, *J*=7.5 Hz, 3H). Mass spectrometry of (R)-outer1_15 confirmed m/z=345.2 [M+H]+. Similarly for (S)-outer1_15 ^{1}H NMR (500 MHz, DMSO-*d*6) showed peaks consistent with the compound's structure: δ 8.68 (d, *J*=43.7 Hz, 1H), 8.26 - 8.04 (m, 2H), 7.65 - 7.50 (m, 1H), 4.56 (dd, *J*=72.1, 9.8 Hz, 2H), 3.77 - 3.64 (m, 1H), 3.49 (d, *J*=6.5 Hz, 1H), 3.10 (s, 2H), 2.80 - 2.59 (m, 2H), 2.22 (d, *J*=24.6 Hz, 2H), 2.00 - 1.80 (m, 2H), 1.67 (ddd, *J*=33.1, 14.2, 7.0 Hz, 3H), 1.05 (t, *J*=7.5 Hz, 3H). Mass spectrometry of (S)-outer1_15 confirmed m/z=345.2 [M+H]+.

Supplementary References

1. K. Bettayeb, *et al.*, Meriolins, a new class of cell death inducing kinase inhibitors with enhanced selectivity for cyclin-dependent kinases. *Cancer Res.* **67**, 8325–8334 (2007).

2. X. Wang, *et al.*, Identification of MRTX1133, a Noncovalent, Potent, and Selective KRASG12D Inhibitor. *J. Med. Chem.* **65**, 3123–3133 (2022).